Journal of Pharmaceutical and Biomedical Analysis 49 (2009) 64–71

Contents lists available at ScienceDirect

Journal of Pharmaceutical and Biomedical Analysis

journal homepage: www.elsevier.com/locate/jpba

Shell and small particles; Evaluation of new column technology

Szabolcs Fekete[a,*], Jenő Fekete[b], Katalin Ganzler[a]

[a] Formulation Development, Gedeon Richter Plc, Gyömrői út 19-21, Budapest X., Hungary
[b] Budapest University of Technology and Economics, Department of Inorganic and Analytical Chemistry, Szt. Gellért tér 4, Budapest 1111, Hungary

ARTICLE INFO

Article history:
Received 11 August 2008
Received in revised form
29 September 2008
Accepted 6 October 2008
Available online 22 October 2008

Keywords:
Column efficiency
Shell particles
Peak capacity
Kinetic plot
Ascentis Express

ABSTRACT

The performance of 5 cm long columns packed with shell particles was compared to totally porous sub-2 μm particles in gradient and isocratic elution separations of hormones (dienogest, finasteride, gestodene, levonorgestrel, estradiol, ethinylestradiol, noretistherone acetate, bicalutamide and tibolone). Peak capacities around 140–150 could be achieved in 25 min with the 5 cm long columns. The Ascentis Express column (packed with 2.7 μm shell particles) showed similar efficiency to sub-2 μm particles under gradient conditions. Applying isocratic separation, the column of 2.7 μm shell particles had a reduced plate height minimum of approximately $h = 1.6$. It was much smaller than obtained with totally porous particles ($h \approx 2.8$). The impedance time also proved more favorable with 2.7 μm shell particles than with totally porous particles. The influence of extra-column volume on column efficiency was investigated. The extra-column dispersion of the chromatographic system may cause a shift of the HETP curves.

1. Introduction

In liquid chromatography a new age has started with using sub-2 μm particles, monolith columns and shell particles. The theory of Van Deemter and his well-known equation [1] paved the way to get higher plate numbers and better resolution in separation. On sub-2 μm particles, due to the narrow peaks, sensitivity and separation are improved albeit at the cost of pressure. Extra-column effects are more significant for scaled down separations, therefore it is essential to minimize extra-column dispersion. It took many years to introduce the theoretical approach into practice. The first fast and dedicated system for ultra-high-pressure separation was released in the year of 2004. The new hardware was able to work up to 1000 bar (15,000 psi) and the particle size of stationary phases was reduced down to 1.7 μm. To distinguish this new technology from conventional high-performance liquid chromatography (HPLC) a new name, ultra-performance liquid chromatography (UPLC) was introduced. It was proved that the analysis time could be reduced down to a 1- or 2-min interval without the loss of resolution and sensitivity [2,3].

One solution to moderate ultra-high pressure ($P > 400$ bar) is to elevate temperature. Analysis time can also be shortened without the loss of resolution through column heating [4–7]. Mobile phase viscosity decreases with increasing temperature and, thus, column back-pressure decreases. Systems with a maximum pressure capability of 400 bar can then be used with the sub-2 μm columns without over-pressuring the pump. Preheating of the mobile phase is essential to avoid brand broadening.

Monolithic columns are attractive alternatives to packed columns. Like other continuous media, monolithic columns approach fast analysis by bypassing the limitations imposed by pressure via through-pores, which allow higher flow rates than particulate columns at reasonable column back-pressure. Analyte retention is usually provided within the monolithic structure by smaller mesopores. This monolith approach, originally initiated by the work of Hjertén et al. [8], Svec and Frechet [9], Horvath and co-workers [10] and Tanaka and co-workers [11], which already lead to a number of well-performing, commercially available polymeric and silica monolith columns [12,13].

Another approach dates back to the early days of liquid chromatography. Horvath and co-workers [14,15] first demonstrated pellicular particles, made of a solid core surrounded by a layer of porous material. This medium became the first commercial HPLC packing that provided convincing results. Horvath at al. also suggested the pellicular type stationary phases for the separation of biopolymers. Later Kirkland [16] developed similar products that were useful in liquid–liquid chromatography and liquid–solid (adsorption) chromatography. The most recent introduction of a superficially porous particle is the so-called fused-core particle [17,18]. The outer shell is sufficiently thin (0.50 μm) to allow rapid mass transfer into and out of the stationary phase; because the inner core is solid, analytes cannot penetrate any further. This

* Corresponding author.
E-mail address: fekete.szabolcs1@chello.hu (S. Fekete).

0731-7085/$ – see front matter © 2008 Elsevier B.V. All rights reserved.
doi:10.1016/j.jpba.2008.10.009

diffusion path length is shorter than in the porous particles of approximately the same diameter and roughly equivalent to the sub-2 μm particles.

In this study the effectiveness of sub-2 μm totally porous particles and porous silica layered solid core type (2.7 μm) particles were compared under isocratic and gradient elution conditions. We also tried to compare the extra-column dispersion of dedicated UPLC and other fast and conventional HPLC systems when small columns packed with porous and shell particles are applied. The test analytes were steroids and a non-steroidal hormone (polar neutral compounds), which are used as a treatment in contraception, climax, prostatic hyperplasia, prostate cancer and hirsutism. Comparison of shell particles to other porous particles is a favorable topic [17,19] but according to our best knowledge there is no such study in which the peak capacity, Van Deemter plots, and other kinetic plots of 1.5, 1.7, 1.9 μm, totally porous particles and porous silica layered solid core type (2.7 μm) particles are compared.

2. Experimental

2.1. Chemicals, column

Acetonitrile and methanol (gradient grade) were purchased from Merck (Darmstadt, Germany). For measurements water was prepared freshly using Milli-Q equipment (Milli-Q gradient A10 by Millipore).

The reference materials and samples as dienogest (17α-cyanomethyl-17β-hydroxyestra-4,9(10)-diene-3-one), finasteride (*N*-*tert*-butyl-3-oxo-4-aza-5α-androst-1-ene-17β-carboxamide), gestodene (13-ethyl-17-hydroxy-18,19-dinor-17α-pregna-4,15-dien-20-yn-3-one), levonorgestrel (13-ethyl-17-hydroxy-18,19-dinor-17α-pregn-4-en-20-yn-3-one, (−)), estradiol (estra-1,3,5(10)-triene-3,17β-diol), ethinylestradiol (19-nor-17-pregn-1,3,5(10)-trien-20-yn-3,17-diol), noretistherone acetate (17-acetoxy-19-nor-17α-pregn-4-en-20-yn-3-one), bicalutamide (*N*-[4-cyano-3-(trifluoromethyl)phenyl]-3-(4-fluorophenyl)sulfonyl)-2-hydroxy-2-methyl propanamide, (±)), and tibolone (17-hydroxy-7α-methyl-19-nor-17α-pregn-5(10)-en-20-yn-3-one) were produced by Gedeon Richter Plc (Budapest, Hungary).

Ascentis Express C18 column (Supelco) with a particle size of 2.7 μm (50 mm × 2.1 mm) was purchased from Sigma–Aldrich Ltd., Budapest. Waters UPLC™ BEH C18 column with a particle size of 1.7 μm (50 mm × 2.1 mm) was purchased from Waters Ltd., Budapest. Grace Vision HT C18 column with a particle size of 1.5 μm (50 mm × 2.0 mm) was purchased from Lab-Comp Ltd., Budapest. Hypersil Gold C18 column (Thermo) with a particle size of 1.9 μm (50 mm × 2.1 mm) was purchased from Lab-Comp Ltd., Budapest.

2.2. Equipment, softwares

Throughout the measurements a Waters Acquity UPLC™ (ultra-performance liquid chromatography) system with Empower software from Waters Ltd., Budapest, Hungary, a Shimadzu UFLC (ultra-fast liquid chromatography) Prominence system with Class VP software from Simkon Ltd., Budapest, Hungary and an Agilent 1200 RRLC (rapid resolution liquid chromatography) system with Chemstation software were employed. Calculation and data transferring to obtain the kinetic plots was achieved by using the Kinetic Method Plot Analyzer template (Gert Desmet, Vrije University Brussel, Belgium). Solvent optimization was performed using Dry Lab 2000 Plus chromatography optimization software (Molnar-Institute Berlin, Germany). Image-J (freeware image-processing software program developed at the National Institutes of Health) was used to determine the particle size distribution of column packing materials.

2.3. Apparatus and methodology

The mobile phases were prepared by mixing appropriate amount of HPLC gradient grade acetonitrile and Milli-Q water. The mixtures were degassed by sonication for 5 min.

The stock solutions of reference standards (dienogest, finasterid, gestodene, levonorgestrel, estradiol, ethinylestradiol, noretisterone acetate, bicalutamide and tibolone) were dissolved in methanol (1000 μg/ml). The solutions for the chromatographic runs were diluted from the stock solutions with acetonitrile/water 40/60 (v/v). The concentration of the test analytes was 10 μg/ml.

For the measurement of peak capacity, gradients with different time (5, 10, 15, 20 and 25 min) were run from 10% to 80% acetonitrile. For this study 35 and 60 °C column temperature, 0.5 ml/min flow rate, 0.5 μl injection and detection at 220 nm were applied.

The kinetic efficiency of the columns were determined with a mobile phase contained 40% acetonitrile in case of all columns, 35 °C column temperature, 0.5 μl injection and detection at 220 nm were applied. The flow rate was varied from 0.05 up to 1.0 ml/min.

2.4. Equations used for calculation

Peak capacity defines a measure of the column performance under gradient conditions. Several definitions and equations are used for the determination of peak capacity [20–22]. One of those is conditional peak capacity, which can be calculated with very simple formulas, which use the data of obtained chromatograms, such as retention times, average peak width and gradient duration time.

In this study we used the following equation to determine peak capacity:

$$n_c^* = 1 + \frac{t_G}{w}$$

where t_g is the gradient duration, and w is the average peak width.

The column efficiency is mostly illustrated by the Van Deemter curves. Previously Desmet et al. showed [23,24] that it is very straightforward to map the kinetic performance of a given chromatographic support type by taking a representative set of the Van Deemter curve data and re-plotting them as H^2/K_{V0} versus $K_{V0}/(uH)$ instead of H versus u. The minimal analysis time can be calculated by simple rearranging the data in a measured Van Deemter curve and the value of the column permeability (K_{V0}). The following equations transform the linear velocity–plate height data into t_0 time versus plate number (N).

$$N = \frac{\Delta P}{\eta}\left(\frac{K_{V0}}{u_0 H}\right)$$

$$t_0 = \frac{\Delta P}{\eta}\left(\frac{K_{V0}}{u_0^2}\right)$$

where N is the plate number, η mobile phase viscosity, ΔP available pressure drop, K_{V0} column permeability, u_0 linear velocity, and H is the plate height. The obtained values correspond directly to the minimal t_0 time needed in a column taken exactly long enough to yield a given number of theoretical plates. It is easy to combine the given N value with the corresponding plate height value to obtain the corresponding column length.

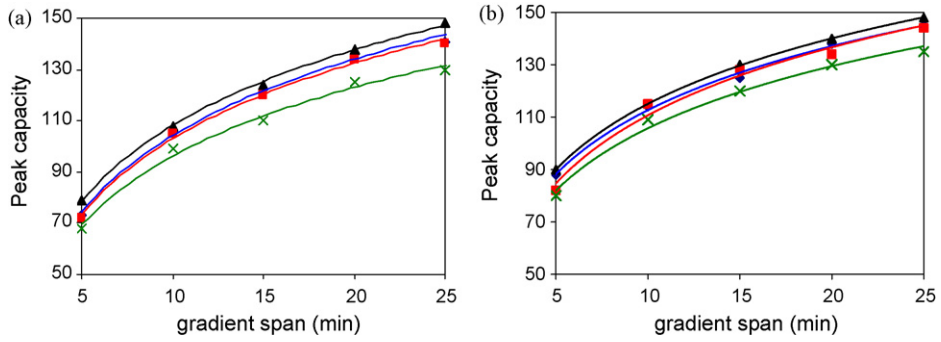

Fig. 1. Peak capacity curves at (a) 35 °C, (b) 60 °C of 2.7 μm shell and sub-2 μm totally porous particles. Mobile phase: acetonitrile–water gradient; flow: 0.5 ml/min; injection: 0.5 μl; solute: mixture of nine hormone compounds. (▲) Black curve: Grace Vision HT C18 column with a particle size of 1.5 μm (50 mm × 2.0 mm); (■) red curve: Waters UPLCTM BEH C18 column with a particle size of 1.7 μm (50 mm × 2.1 mm); (×) green curve: Hypersil Gold C18 column with a particle size of 1.9 μm (50 mm × 2.1 mm); (♦) blue curve: Ascentis Express C18 column (Supelco) with a particle size of 2.7 μm (50 mm × 2.1 mm). (For interpretation of the references to color in this figure legend, the reader is referred to the web version of the article.)

The most common type of kinetic plot represents t_0/N^2 values as a function of N [25]:

$$\frac{t_0}{N^2} = \frac{\eta}{\Delta P}\left(\frac{H^2}{K_{V0}}\right) = \left(\frac{\eta}{\Delta P}\right) E_0 = t_E$$

where E_0 is defined as the separation impedance number [26]. The time required to obtain a certain resolution for a separation, with a specific pressure drop, is directly proportional to the separation impedance of the column. The lower the separation impedance, the better is the performance of the column. Plotting t_0/N^2 ratio as a function of N and reversing the direction of the N axis, the obtained impedance time plots still represent the same kinetic information as the plot of t_0 versus N, but regain the familiar view of a conventional Van Deemter curve.

3. Results and discussion

3.1. Peak capacity

At first for a basic comparison peak capacity curves were measured for all four columns. The injected sample contained nine hormone compounds (10 μg/ml) diluted with acetonitrile/water 40/60 (v/v). The measurements were carried out with the columns kept at constant temperature of 35 and 60 °C. A flow rate of 0.5 ml/min, injection volume of 0.5 μl and detection at 220 nm were applied. For the measurements a Waters UPLC system was applied. Fig. 1 shows the obtained peak capacity curves of the different columns versus the gradient span.

The highest peak capacity could be achieved with the column packed with 1.5 μm totally porous particles. The columns packed with porous 1.7 μm and shell 2.7 μm particles show similar capacity. Peak capacities of about 140–150 could be achieved in 25 min with the 5 cm long column packed with shell particles when steroid compounds are separated.

3.2. Column efficiency

The efficiencies of the four columns used in this work were measured at the temperature of 35 °C by means of the Van Deemter plots. A small amount of levonorgestrel (10 μg/ml) diluted with acetonitrile/water 40/60 (v/v) was injected to acquire the data. This steroid was eluted with the mobile phase composition of acetonitrile/water 40/60 (v/v). Injection volume of 0.5 μl was applied. The flow rate was varied from 0.05 up to 1.0 ml/min. The measurements were carried out on a Waters UPLC system.

Fig. 2(a) shows the obtained HETPs (micrometer) versus the linear velocity while Fig. 2(b) shows the reduced HETPs ($h = H/d_p$), with $H = A + B/u + Cu$, d_p the particle size. The fitting parameters of A, B, C, the calculated u_{opt}, $HETP_{min}$ and h_{min} values are reported in Table 1.

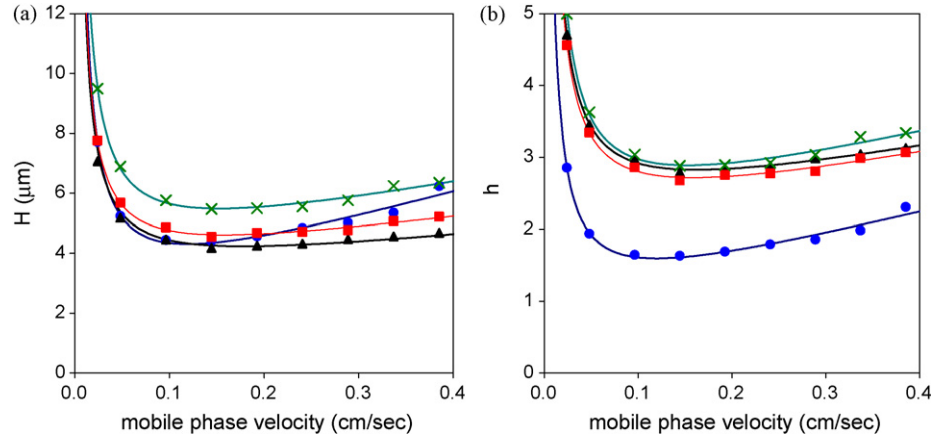

Fig. 2. Experimental Van Deemter (a) and reduced plate height (b) plots of 2.7 μm shell and sub-2 μm totally porous particles (peak widths are corrected for the extra-column broadening). Mobile phase: 40% acetonitrile–60% water; temperature: 35 °C; injection: 0.5 μl; solute: levonorgestrel. (▲) Black curve: Grace Vision HT C18 column with a particle size of 1.5 μm (50 mm × 2.0 mm); (■) red curve: Waters UPLCTM BEH C18 column with a particle size of 1.7 μm (50 mm × 2.1 mm); (×) green curve: Hypersil Gold C18 column with a particle size of 1.9 μm (50 mm × 2.1 mm); (●) blue curve: Ascentis Express C18 column (Supelco) with a particle size of 2.7 μm (50 mm × 2.1 mm). (For interpretation of the references to color in this figure legend, the reader is referred to the web version of the article.)

Table 1
Van Deemter parameters, u_{opt}, $HETP_{min}$ and h_{min} values of levonorgestrel on the four columns at 35 °C.

Parameters	Ascentis Express C18 2.7 μm	Grace Vision C18 1.5 μm	Acquity BEH C18 1.7 μm	Hypersil Gold C18 1.9 μm
A	2.17	3.08	3.28	3.68
B	0.13	0.09	0.11	0.14
C	8.94	3.59	4.23	5.93
u_{opt} (cm/s)	0.12	0.18	0.16	0.15
$HETP_{min}$	4.3	4.2	4.6	5.4
h_{min}	1.6	2.8	2.7	2.8

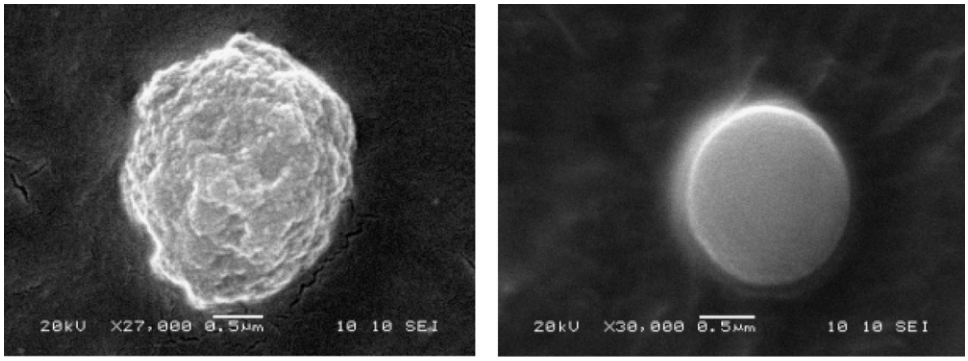

(a) fused core particle (b) sub 2 μm porous particle

Fig. 3. SEM pictures of (a) Ascentis Express shell (fused core) particle and (b) Waters UPLC BEH 1.7 μm porous particle.

The C term for shell particles is about two times higher than for sub-2 μm particles. It can be explained by the rough surface of particles in which the mass transfer rate is reduced through the outer stagnant liquid. Guiochon et al. [19] came to similar result when they compared Halo particles to 3, 3.5 and 5 μm porous particles. Scanning electron microscopy (SEM) pictures of the Ascentis Express and Waters UPLC™ BEH materials are shown in Fig. 3.

The plate height of the 2.7 μm Ascentis Express column is very similar to the HETP of 1.5 and 1.7 μm totally porous particles. The column of 2.7 μm shell particles has a reduced plate height minimum of approximately $h = 1.6$ in this study. The lowest reduced plate height ever reported of columns packed with shell particles (HALO) is about $h = 1.4$ [17]. Columns of the sub-2 μm particles show higher reduced plate values. The three columns packed with totally porous particles display a very similar ($h \approx 2.8$) reduced plate height with the optimum mobile phase velocity between 0.1 and 0.2 cm/s. The very small reduced plate height of the column packed with shell particles can be explained by the shorter diffusion path and by the very narrow particle size distribution [19,27]. SEM images and Image-J (image-processing software) were used to determine the particle size distribution of the Ascentis Express and Waters UPLC™ BEH materials (Fig. 4). However, the efficiency of Ascentis Express column decreases faster with an increasing mobile phase velocity. The optimum of mobile phase velocity is higher when sub-2 μm particles ($u_{opt} \approx 0.15$–0.18 cm/s) are used than in the case of shell particles ($u_{opt} \approx 0.12$ cm/s). The lower optimum linear velocity might also be the consequence of the rough surface of shell particles.

3.3. Kinetic plots

The permeability of the four columns was assessed from the plot of the experimental column pressure (P) versus the flow rate (Fig. 5). Column permeability data, which were used for the calculations of kinetic plots were corrected with system pressure drop (extra-column pressure drop).

The data in a measured Van Deemter curve and the value of the column permeability were used to calculate the kinetic plots. The obtained t_0 time versus required plate number (N) curves are shown in Fig. 6. The column lengths obtained are plotted in Fig. 7. The impedance time plots for the four different type of columns are displayed in Fig. 8. All the kinetic plots related to 400 and 600 bar (5800 and 8700 psi) pressure drop. The maximum allowable pressure with a conventional HPLC system is 400 bar. The Ascentis Express fused core columns are certified up to 600 bar.

The Ascentis Express column (2.7 μm particles) has much higher permeability than sub-2 μm packed columns so it allows the users to achieve fast separations with modest operating pressure.

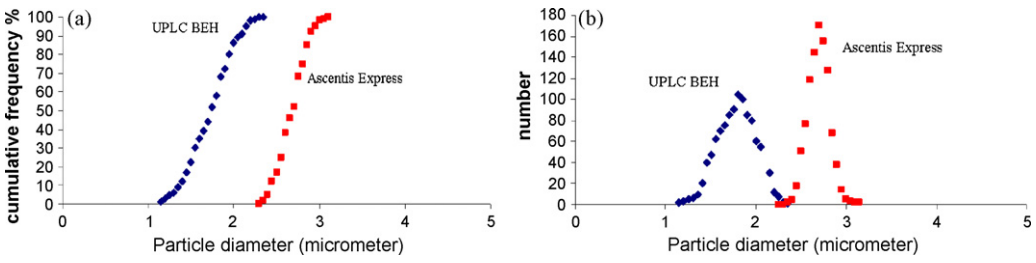

Fig. 4. Cumulative frequency (a) and particle size distribution (b) of Ascentis Express 2.7 μm shell particles and Waters UPLC BEH 1.7 μm porous particles.

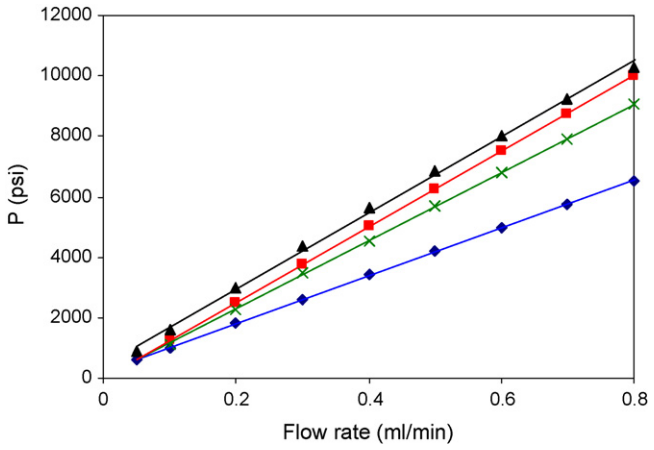

Fig. 5. Column permeability. (▲) Black curve: Grace Vision HT C18 column with a particle size of 1.5 μm (50 × 2.0 mm); (■) red curve: Waters UPLCTM BEH C18 column with a particle size of 1.7 μm (50 mm × 2.1 mm); (×) green curve: Hypersil Gold C18 column with a particle size of 1.9 μm (50 mm × 2.1 mm); (♦) Blue curve: Ascentis Express C18 column (Supelco) with a particle size of 2.7 μm (50 mm × 2.1 mm). (For interpretation of the references to color in this figure legend, the reader is referred to the web version of the article.)

When higher plate number is required (N > 15–20,000) the analysis time is more advantageous in case of 2.7 μm shell particles. If smaller plate number is demanded, the columns packed with small totally porous particles yield shorter analysis time. We found the same trend with column length. The advantage of the shell particles against porous particles can be demonstrated unambiguously with the impedance time plots. Much shorter impedance time can be achieved with 2.7 μm shell particles than with porous particles. However, the impedance time of Ascentis Express column increases faster with decreasing required plate numbers. The optimum of theoretical plate number is smaller when sub-2 μm particles (N_{opt} ≈ 10,000–20,000) are used than in the case of shell particles (N_{opt} ≈ 30,000–40,000).

3.4. Extra-column dispersion effect on column performance

The dispersion of analyte bands in the extra-column volumes can be decomposed into three parts. The contributions to band broadening due to the axial dispersion in the capillary tubes that are swept by the mobile phase stream (Taylor-Aris dispersion) [28], the exponential tailing due the mixer type behavior of those extra-column volumes that are not convectively swept [29] and the finite width of the rectangular injection profile.

Extra-column effects are more significant for scaled down separations (column volume decreases). The following equation shows the achievable improvements in resolution, asymmetry and effi-

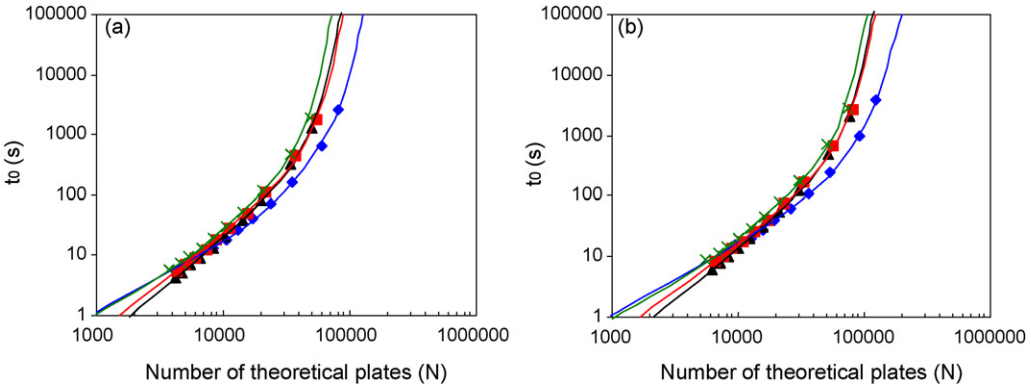

Fig. 6. t_0 vs. N plots with maximum available pressure drop of 400 bar (a) and 600 bar (b). (▲) Black curve: Grace Vision HT C18 column with a particle size of 1.5 μm (50 mm × 2.0 mm); (■) red curve: Waters UPLCTM BEH C18 column with a particle size of 1.7 μm (50 mm × 2.1 mm); (×) green curve: Hypersil Gold C18 column with a particle size of 1.9 μm (50 mm × 2.1 mm); (♦) blue curve: Ascentis Express C18 column (Supelco) with a particle size of 2.7 μm (50 mm × 2.1 mm). (For interpretation of the references to color in this figure legend, the reader is referred to the web version of the article.)

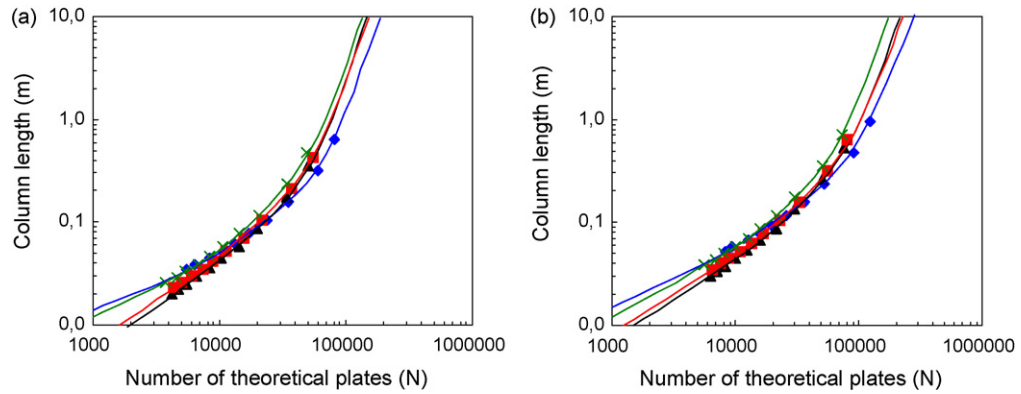

Fig. 7. Column length vs. N plots with maximum available pressure drop of 400 bar (a) and 600 bar (b). (▲) Black curve: Grace Vision HT C18 column with a particle size of 1.5 μm (50 mm × 2.0 mm); (■) red curve: Waters UPLCTM BEH C18 column with a particle size of 1.7 μm (50 mm × 2.1 mm); (×) green curve: Hypersil Gold C18 column with a particle size of 1.9 μm (50 mm × 2.1 mm); (♦) blue curve: Ascentis Express C18 column (Supelco) with a particle size of 2.7 μm (50 mm × 2.1 mm). (For interpretation of the references to color in this figure legend, the reader is referred to the web version of the article.)

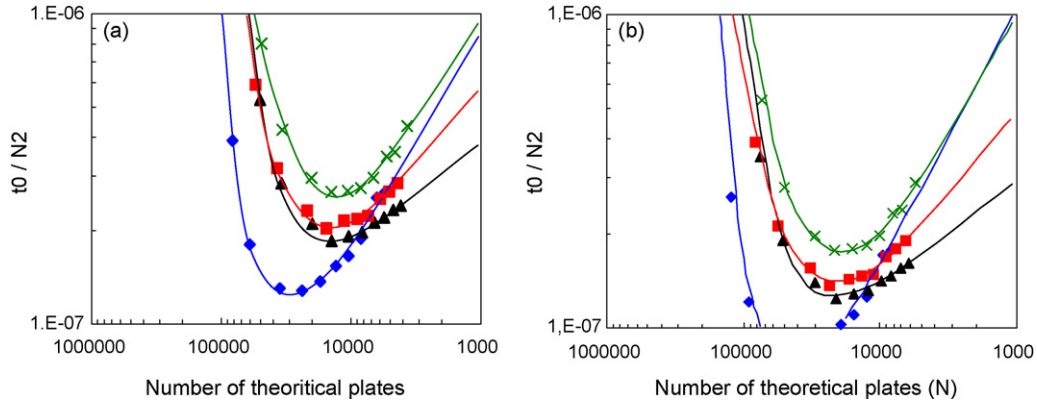

Fig. 8. Impedance time plots with maximum available pressure drop of 400 bar (a) and 600 bar (b). (▲) Black curve: Grace Vision HT C18 column with a particle size of 1.5 μm (50 mm × 2.0 mm); (■) red curve: Waters UPLCTM BEH C18 column with a particle size of 1.7 μm (50 mm × 2.1 mm); (×) green curve: Hypersil Gold C18 column with a particle size of 1.9 μm (50 mm × 2.1 mm); (♦) blue curve: Ascentis Express C18 column (Supelco) with a particle size of 2.7 μm (50 mm × 2.1 mm). (For interpretation of the references to color in this figure legend, the reader is referred to the web version of the article.)

Table 2
Detector cell volume, sampling rate, capillary diameters and extra-column volume of the applied chromatographic systems.

	Waters Acquity UPLC	Agilent 1200 RRLC	Shimadzu Prominence UFLC
Flow cell volume	0.5 μl	2 μl	2.5 μl
Detector data rates	80 Hz	80 Hz	40 Hz
Capillary diameter	0.06 mm	0.12 mm	0.10 mm
Extra-column volume	1.3 μl	2.9 μl	3.7 μl

ciency by reducing the injection volume (V_{inj}), the flow cell volume (V_{cell}) and column to detector connecting tubing internal radius (r_c) [30]:

$$\sigma^2_{ext} \propto K_{inj}\frac{V^2_{inj}}{12} + K_{cell}\frac{V^2_{cell}}{12} + \tau^2F^2 + \frac{r_c^4 \cdot l_c \cdot F}{7.6 \cdot D_m}$$

In addition to the volumetric effects, time constant of the detector (τ, response rate) and scan rate may also contribute to peak broadening; therefore should not be disregarded.

Three different liquid chromatographic systems were compared. The Waters UPLC system, which is dedicated for ultra-high-pressure fast analysis, and other two systems (Agilent 1200 RRLC and Shimadzu Prominence UFLC) which are suggested for fast separation and also for conventional HPLC applications. The detector cell volume and capillary diameters of the applied systems are shown in Table 2. The extra-column band profiles were recorded (Fig. 9) by replacing column with a zero-volume connector and injecting (1 μl) the samples. Levonorgestrel as a test analyte was used for the measurements. A flow rate of 0.5 ml/min was applied for the comparison.

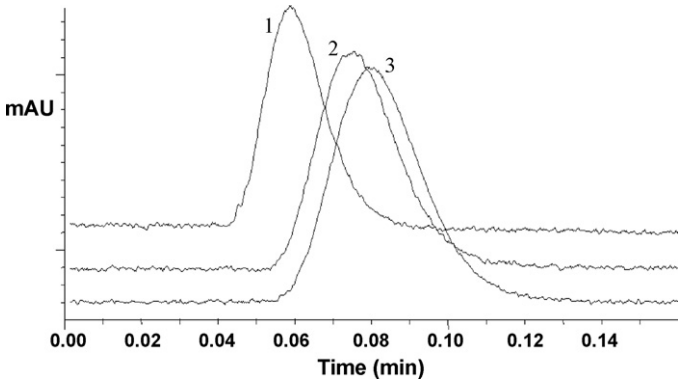

Fig. 9. Extra-column band profiles of the different liquid chromatographic systems. 1: Waters Acquity UPLC; 2: Agilent 1200 RRLC; 3: Shimadzu Prominence UFLC.

Fig. 10 shows the experimental Van Deemter curves obtained on different chromatographic systems to compare the extra-column effects on plate height. The mobile phase contained 40% acetonitrile, 35 °C column temperature and 1 μl injection were applied in the case of all three liquid chromatographic system (Waters Acquity UPLC, Agilent 1200 RRLC and Shimadzu Prominence UFLC). The flow rate was varied from 0.05 up to 1.0 ml/min.

Fig. 10 shows that the instrument and its extra-column dispersion significantly takes effect on the obtained plate heights. It is not enough to observe solely a column's theoretical performance, it is always important to know on which chromatographic system it was applied for. In our example the minimum plate height measured on Ascentis Express column was $HETP_{min}$ = 4.3 (reduced plate height h = 1.6) when measured on dedicated Waters Acquity UPLC system. The Measuring of the Van Deemter curves with Agilent 1200 RRLC system resulted in a minimum plate height of 4.6. In the case of Shimadzu Prominence UFLC system it was 4.7. We assume that these results come from the fact, that the extra-column dispersion is the smallest in the case of the Acquity UPLC system, which is dedicated for ultra-fast analysis. Extra-column effects are more significant, when systems suggested for both conventional and fast separation (Agilent 1200 RRLC and Shimadzu Prominence UFLC), are applied.

Similar tendency of extra-column dispersion was observed when other small columns were compared with different dedicated liquid chromatographic systems. Fig. 10(b) shows the Van Deemter curves obtained with Waters Acquity BEH column. The measured HETP values are 4.6 (Waters Acquity UPLC), 5.0 (Agilent 1200 RRLC) and 5.1 (Shimadzu Prominence UFLC).

3.5. Separation of hormones on shell particles, representative chromatogram

The nine model compounds can be separated with baseline resolution on all of the investigated columns within 2–3 min. Using the same mobile phase (acetonitrile–water) the analysis time depends

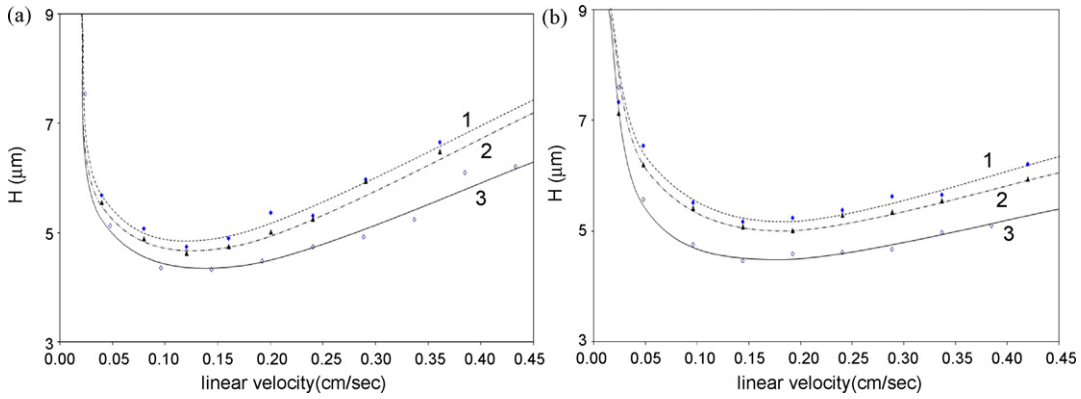

Fig. 10. Experimental Van Deemter curves obtained on different liquid chromatographic systems (a) column: Ascentis Express C18 5 cm × 2.1 mm, 2.7 μm shell particles, (b) Waters Acquity BEH C18, 1.7 μm totally porous particles, test analyte: levonorgestrel. 1: Shimadzu Prominence UFLC; 2: Agilent 1200 RRLC; 3: Waters Acquity UPLC.

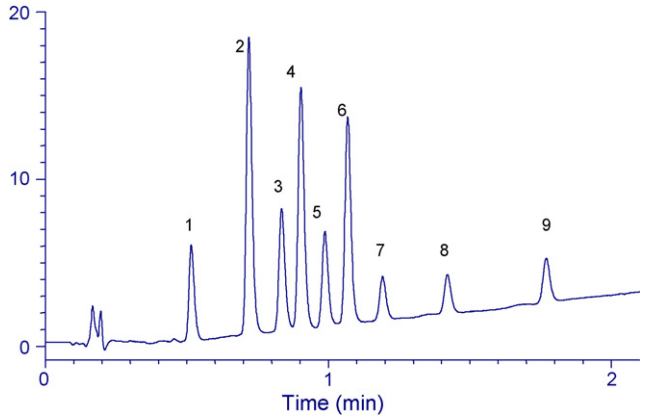

Fig. 11. Chromatogram of model sample. Chromatographic conditions: Ascentis Express C18 2.7 μm (50 mm × 2.1 mm) column; mobile phase: acetonitrile–water gradient elution (35–60% AcN, in 2 min); flow: 0.5 ml/min; column temperature: 20 °C; injection volume: 2 μl; detection: 220 nm. Compounds: (1) dienogest (0.46 μg/ml), (2) estradiol (0.46 μg/ml), (3) finasteride (0.25 μg/ml), (4) ethinylestradiol (0.40 μg/ml), (5) gestodene (0.48 μg/ml), (6) bicalutamide (0.30 μg/ml), (7) levonorgestrel (0.48 μg/ml), (8) tibolone (0.48 μg/ml) and (9) noretistherone acetate (0.46 μg/ml).

on the selectivity of stationary phases. (In this study we have not intended to compare the selectivity of the phases, we investigated only the efficiency of the columns.)

An example is presented for hormone separation using a fused core column (Ascentis Express C18 2.7 μm, 50 mm × 2.1 mm). Throughout the measurements a Waters Acquity UPLC™ system was employed.

Initial four input experiments (gradient time–column temperature model) were performed to optimize the separation on Ascentis Express column. Linear gradients with 6 and 18 min (0.5 ml/min) at 20 and 60 °C column temperature were run. DryLab software was used to predict the optimal solvent ratio and gradient program, which would give a baseline resolution (Rs > 1.5). A fast, gradient method can separate the nine compounds within 2 min (Fig. 11).

4. Conclusion

The Ascentis Express columns packed with 2.7 μm fused core particles (solid cores and 0.5 μm thick porous shell of 9 nm) offer a really high-separation power with modest operating pressure. The performance achieved under both gradient and isocratic condition, is comparable to those obtained with totally porous sub-2 μm particles. Peak capacities around 140–150 could be achieved in 25 min with the 5 cm long columns. In this study the highest plate number was reached with shell particles when polar neutral hormones were separated. The column of shell particles provided a reduced plate height minimum of approximately $h = 1.6$. The impedance time of shell column was also quite favorable compared to other porous particles. Columns packed with fused core particles are worthy of rivaling to any other column packed with sub-2 μm particles.

The influence on the apparent column efficiency of extra-column volume is very important when the performance of small columns (5 cm × 2.1 mm) is compared. The extra-column dispersion of the HPLC system may cause a shift of the HETP curves.

Acknowledgement

The authors wish to thank Imre Pozsgai (Formulation Development, Gedeon Richter Plc) for the scanning electron microscopy (SEM) measurements, pictures and particle size analysis.

References

[1] J.J. Van Deemter, F.J. Zuiderweg, A. Klinkenberg, Chem. Eng. Sci. 5 (1956) 271–289.
[2] M.E. Swartz, B. Murphy, Am. Lab. 37 (2005) 22–35.
[3] M.E. Swartz, J. Liq. Chromatogr. 28 (2005) 1253–1263.
[4] J.A. Blackwell, W.P. Carr, J. Liq. Chromatogr. 14 (1991) 2875–2889.
[5] C. Zhu, D.M. Goodall, S.A.C. Wren, LC–GC N. Am. 23 (2005) 1–9.
[6] H.A. Claessens, M.A. van Straten, Reduction of Analysis Times in HPLC at Elevated Column Temperatures, Eindhoven University of Technology, 2004.
[7] P.T. Jackson, P.W. Carr, Chemtech 28 (1988) 29–37.
[8] S. Hjertén, J.L. Liao, R. Zhang, J. Chromatogr. 473 (1989) 273–275.
[9] F. Svec, J.M. Frechet, J. Anal. Chem. 64 (1992) 820–822.
[10] I. Gusev, X. Huang, C. Horvath, J. Chromatogr. A 885 (1999) 273–290.
[11] H. Minakuchi, H. Nagayama, N. Soga, N. Ishizuka, N. Tanaka, J. Chromatogr. A 797 (1998) 121–131.
[12] H. Oberacher, A. Premstaller, C.G. Huber, J. Chromtogr. A 1030 (2004) 2001–2008.
[13] T. Ikegami, E. Dicks, H. Kobayashi, H. Morisaka, D. Tokuda, K. Cabrera, N. Tanaka, J. Sep. Sci. 27 (2004) 1292–1302.
[14] C. Horvath, S.R. Lipsky, Anal. Chem. 41 (1969) 1227–1234.
[15] C. Horvath, B.A. Preis, S.R. Lipsky, Anal. Chem. 39 (1967) 1442–1451.
[16] J.J. Kirkland, Anal. Chem. 41 (1969) 218–220.
[17] F. Gritti, A. Cavazzini, N. Marchetti, G. Guiochon, J. Chromatogr. A 1157 (2007) 289–303.
[18] N. Marchetti, G. Guiochon, J. Chromatogr. A 1176 (2007) 206–216.
[19] F. Gritti, G. Guiochon, J. Chromatogr. A 1166 (2007) 30–46.
[20] C. Horvath, S.R. Lipsky, Anal. Chem. 39 (1967) 1893–1899.
[21] P.J. Schoenmakers, G. Vivó-Truyols, W.M.C. Decrop, J. Chromatogr. A 1120 (2006) 282–290.
[22] X. Wang, D.R. Stoll, P.W. Carr, P.J. Schoenmakers, J. Chromatogr. A 1125 (2006) 177–181.

[23] G. Desmet, LC–GC Europe 21 (2008) 310–320.
[24] G. Desmet, D. Cabooter, P. Gzil, H. Verelst, D. Mangelins, Y.V. Heyden, D. Clicq, J. Chromatogr. A 1130 (2006) 158–166.
[25] J. Cazes, R.P.W. Scott, Chromatography Theory, Marcel Dekker, New York, 2002.
[26] P.A. Bristow, J.H. Knox, Chromatographia 6 (1977) 279–288.
[27] J.J. DeStefano, T.J. Langlois, J.J. Kirkland, J. Chromatogr. Sci. 46 (2008) 254–260.
[28] G. Taylor, Proc. R. Soc. A186 (1953) 317–319.
[29] A. Felinger, Data Analysis, Signal Processing in Chromatography, Elsevier, Amsterdam, 1998.
[30] F. Gritti, A. Felinger, G. Guiochon, J. Chromatogr. A 1136 (2006) 57–72.